

EFFECT OF NIOBIUM AND MOLYBDENUM ON PHASE TRANSFORMATIONS IN ADVANCED LOW-CARBON STEELS

M. Militzer, F. Fazeli and T. Jia

The Centre for Metallurgical Process Engineering,
The University of British Columbia,
Vancouver, BC, Canada V6T 1Z4

Keywords: X65, X80, Phase Transformation, Linepipe, Solute Drag, Niobium, Molybdenum, CCT, Thermal Simulation, Modelling, Kinetics

Abstract

Advanced high strength steels are frequently microalloyed with Nb and/or Mo. Both elements are known to have a tremendous effect on the austenite-ferrite transformation, which constitutes the key metallurgical tool to tailor the properties. The effects of Nb on the continuous cooling transformation behavior are quantified for two linepipe steels by separately controlling the austenite grain size and the content of Nb in solution. One of the investigated steels is an X80 grade that also contains Mo and the transformation studies are used to quantify the synergistic role of Nb and Mo. Bringing Nb into solution decreases the transformation temperature by up to 100 °C for accelerated cooling conditions. The experimental results are described in the framework of phenomenological models for the austenite-to-ferrite transformation. In particular the effect of Nb and Mo on the apparent austenite-ferrite interface mobility is analyzed.

Introduction

The use of Nb and Mo is a critical aspect for developing advanced low carbon high strength steels, e.g. for automotive and pipeline applications. Over the past 60 years Nb has increasingly been employed as a microalloying element to engineer state-of-the-art flat and bar products [1,2,3]. Adding Nb is particularly effective in refining ferrite microstructures but Nb may also act as a precipitation strengthener when fine Nb(CN) precipitates form. One of the striking features of Nb addition is the increase of the austenite recrystallization temperature and this is utilized in thermo-mechanical controlled processing [4,5,6]. Furthermore, Nb in solution promotes formation of acicular ferrite constituents and shifts austenite decomposition to lower temperatures [6,7,8]. The effect on phase transformation is very profound, such that only a few ppm of dissolved Nb changes the decomposition kinetics dramatically. The amount of dissolved Nb at the onset of the austenite decomposition may potentially differ from the nominal Nb content of the steel depending on the processing conditions. For example, in plate rolling some of the Nb may precipitate in austenite whereas this is less likely in strip rolling due to shorter processing times. Despite these important industrial implications and a significant body of research work including numerous experimental observations, the influence of Nb in solution on austenite decomposition has yet to be quantified unambiguously, [9,10,11]. In particular, the role of systematically varied Nb levels in solution needs to be quantified for a given steel chemistry to exclude potential additional effects on phase transformation when taking the more traditional approach of studying a number of steels with different Nb contents.

Mo is another element with a major effect on the austenite decomposition kinetics. There is a large body of work on the effect of Mo on the transformation kinetics showing that Mo delays the ferrite formation, can lead to incomplete transformation and, as a result, the separation of the ferrite and bainite portions in the overall transformation through the emergence of the bainite bay in the time-temperature-transformation diagrams with increasing Mo content [12,13]. Thus, adding Mo is a very efficient strategy to tailor the phase transformation such that under the constraints of an industrial processing line the desired multi-phase microstructure can be formed that is required to attain the property targets of the steel product [14]. Similar to Nb, Mo also delays the recrystallization in ferrite and austenite. Even though many steels contain both Nb and Mo, there is surprisingly little quantitative information on their combined effects on the austenite decomposition kinetics [15,16].

The present paper describes systematic studies to quantify the effect of Nb in solution on ferrite formation in two Nb microalloyed linepipe grades, one of which is also alloyed with Mo. A novel experimental methodology permits to vary the content of dissolved Nb in austenite while maintaining an invariant austenite grain size. Recording the subsequent decomposition kinetics of austenite enables quantification of the role of various Nb contents in solution. Based on the experimental observations, a solute drag parameter for Nb is incorporated into a model for the ferrite transformation-start temperature during continuous cooling. Further, the effect of Nb on the migration rate of the ferrite-austenite interface is analyzed in terms of an apparent interface mobility.

Materials and Experimental Methodology

The current study includes two commercial linepipe steel grades, i.e. an X65 and an X80 steel both microalloyed with Nb. The steel chemistries are shown in Table I. The X80 steel contains also Mo as an alloying addition. The A_{e3} temperatures of these two steels are 839 °C and 823 °C, respectively, as determined by Thermo-Calc using the Fe2000 data-base. From these materials two types of samples were machined for continuous cooling transformation (CCT) studies, i.e. tubular specimens with a wall thickness of 1 mm when no deformation step is included in the test procedures and, for tests with deformation, solid samples having a cylindrical working zone with a 6 mm diameter.

Table I. Chemical Composition of Investigated Steels (Key Elements in wt%)

Steel	C	Mn	Nb	Ti	Mo	N
X65	0.06	1.49	0.047	-	-	0.0094
X80	0.06	1.65	0.034	0.012	0.24	0.005

The CCT tests were conducted in a Gleeble 3500 thermo-mechanical simulator equipped with a dilatometer. To study the effect of Nb in solution on the phase transformation kinetics, austenitizing treatment schedules were developed that enabled independent variation of the austenite grain size and the amount of Nb in solution. For the X65 steel a thermo-mechanical treatment was employed that replicates key features of a hot rolling process, as shown in Figure 1. First, the samples were reheated at 1200 °C for 2 mins to bring all Nb into solution. This was followed by a deformation step in compression (true strain of 0.3) at 1050 °C to refine the austenite grain size through recrystallization. An average austenite grain size of 40 μm

resulted from this thermo-mechanical treatment. The deformation conditions at 1050 °C were selected to avoid re-precipitation of Nb. Then, the samples were cooled at 100 °C/s to 900 °C where they were held for selected times to obtain different levels of re-precipitation of Nb and, thus, different amounts of Nb in solution. Austenite grain growth during the holding at 900 °C is negligible. The amount of Nb in solution was estimated from a precipitation study by Park et al. [17], on a steel with a similar chemistry (0.08 wt% C, 1.21 wt% Mn, 0.038 wt% Nb, 0.0017 wt% N), i.e. 281 ppm at 0 min (all Nb in solution), 230 ppm at 2 mins and 44 ppm at 20 mins, respectively.

For the X80 steel, a similar re-precipitation step was conducted at 900 °C after having brought all Nb in solution but without a deformation step, i.e. employing thermal cycles that are similar to those in the weld heat affected zone (HAZ). For CCT studies with larger austenite grain sizes (here 26 µm) the samples were directly cooled from a suitable reheat condition (here 5 s at 1250 °C) to 900 °C, see Figure 2(a), whereas for smaller austenite grain sizes a two-step reheating procedure can be employed, see Figure 2(b). Here the sample is quenched from the solution temperature to room temperature and then quickly reheated to a selected temperature in austenite (e.g. 950 °C for a grain size of 5 µm) before conducting the precipitation heat treatment at 900 °C. Even though the Nb content in the X80 steel is similar to that in the steel studied by Park et al. [17], the precipitation kinetics are expected to be different due to the presence of Ti and Mo. In particular, the addition of Mo reduces the rate of Nb(CN) precipitation in austenite [18]. Thus, systematic age hardening studies were performed at 610 °C for samples that had been exposed to different holding times at 900 °C. The peak strength increment observed in these aging experiments was taken as a measure of the apparent volume fraction of Nb precipitated during aging. From this volume fraction one can estimate the amount of Nb that was in solution before aging, i.e. that had not been precipitated at 900 °C. From these studies it was concluded that the degree of re-precipitation of Nb was approximately 64% after 20 mins holding at 900 °C which is significantly less than in the X65 steel (93%). Then, the following Nb levels in solution were adopted for the X80 steel: 204 ppm for 0 mins and 73 ppm for 20 mins holding at 900 °C.

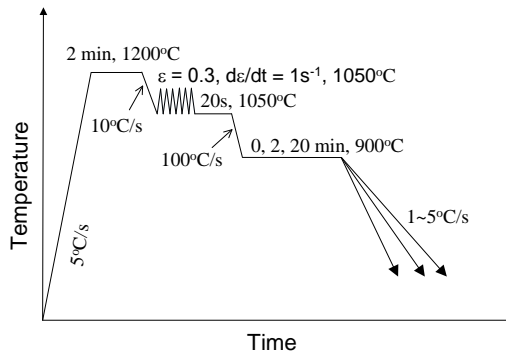


Figure 1. Thermo-mechanical processing path of CCT tests for X65 steel.

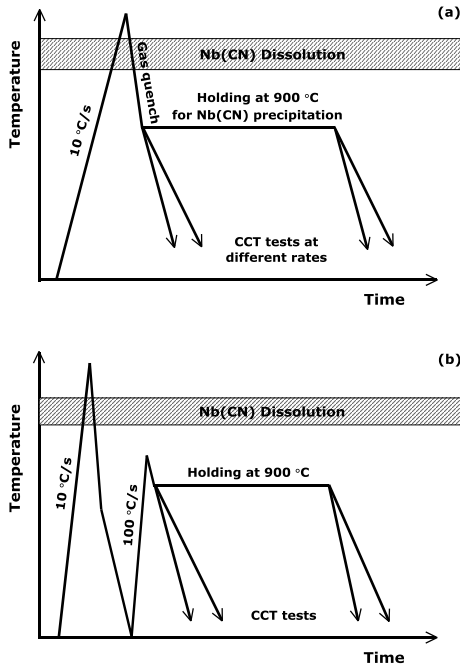


Figure 2. Processing paths for CCT tests in X80 steel; (a) large austenite grain size, (b) small austenite grain size.

Experimental Results

Effect of Nb on the Austenite-to-Ferrite Transformation

Figure 3 shows the austenite decomposition kinetics in the X65 steel as a function of temperature during cooling at 5 °C/s. Having more Nb in solution systematically lowers the transformation temperatures. Considering the cases of 20 min holding at 900 °C vs no holding, i.e. almost full re-precipitation of Nb vs all Nb in solution, shows a decrease of transformation temperatures of about 50 °C in the initial transformation stages of up to 50% transformed when bringing all Nb in solution. The microstructures obtained in these two CCT tests are shown in Figure 4. For the higher transformation temperature (i.e. Nb re-precipitated) a fine grained ferrite structure is observed with a mixture of polygonal and irregular grains; these ferrite structures are often termed as “acicular ferrite” even though the ferrite may not form on inclusions or large precipitates for which a truly acicular growth had first been observed. In the case of Nb in solution where the transformation is shifted to lower temperatures, the resulting microstructure is a clear mixture of polygonal ferrite that has formed at prior austenite grain boundaries and

bainitic ferrite inside the prior austenite grains. The ferrite fractions for the three cases shown in Figure 3 increase from 0.25 to 0.31 and 0.47 when reducing the Nb level in solution by increasing the holding time at 900 °C. These experimental observations provide further evidence that Nb in solution delays the ferrite formation thereby promoting a more bainitic microstructure for a given cooling condition in the investigated steel.

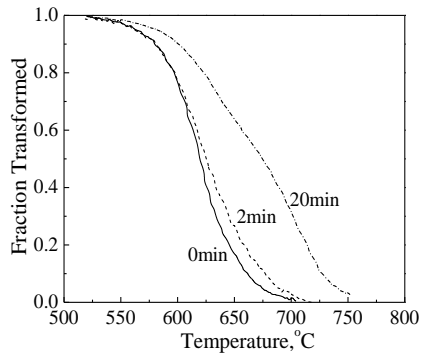


Figure 3. Effect of Nb in solution on the austenite decomposition kinetics in the X65 steel cooled at 5 °C/s.

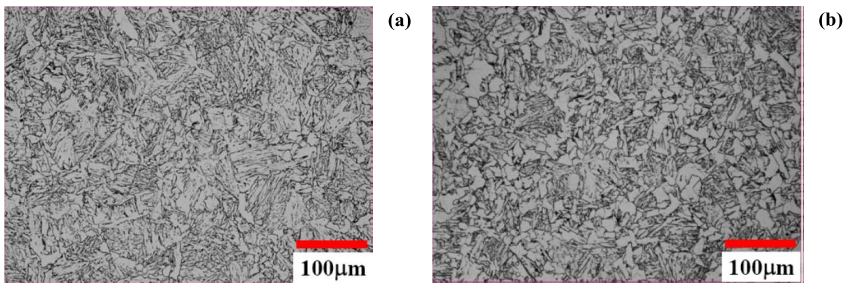


Figure 4. Microstructures in the X65 steel when cooled at 5 °C/s for (a) Nb in solution (no holding at 900 °C) and (b) Nb re-precipitated (20 min holding at 900 °C).

Effect of Nb and Mo on the Austenite-to-Ferrite Transformation

In the X80 steel a similar trend as in the X65 steel was observed for the effect of Nb in solution on the austenite decomposition kinetics. Increasing the amount of Nb in solution delays the transformation and lowers the transformation temperature. As illustrated in Figure 5, the transformation temperature can be lowered by approximately 100 °C for accelerated cooling conditions with a cooling rate of 30 °C/s and a prior austenite grain size of 5 μm . The resulting microstructures are shown in Figure 6. Lowering the transformation temperature leads to a transition from a fine-grained polygonal ferrite microstructure to a fine-grained but more irregular ferrite microstructure with an increased fraction of bainitic ferrite. In both cases randomly distributed fine martensite/austenite (M/A) islands are observed with an average size of approximately 1 μm .

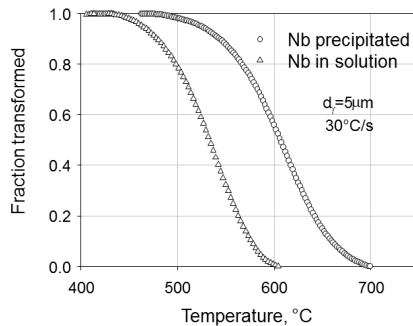


Figure 5. Effect of Nb in solution on the austenite decomposition kinetics in the X80 steel with a prior austenite grain size of 5 μm cooled at 30 °C/s.

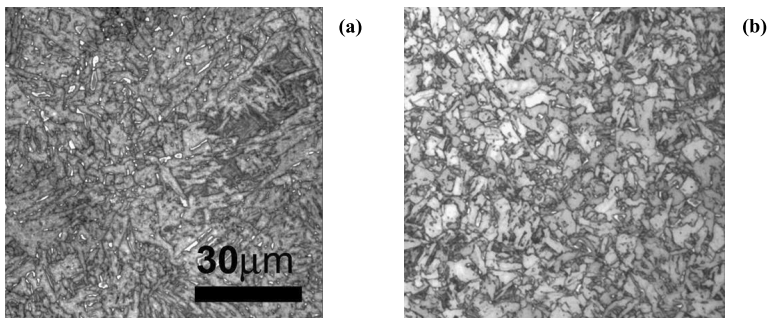


Figure 6. Microstructures in the X80 steel with a prior austenite grain size of 5 μm cooled at 30 °C/s for (a) Nb in solution (no holding at 900 °C) and (b) Nb re-precipitated (20 min holding at 900 °C).

The role of Nb may in detail be somewhat different than in the X65 steel since in the X80 steel Mo is also present in solution. Mo is known to similarly delay the ferrite formation. To evaluate potential synergistic effects of Nb and Mo on the kinetics of the austenite-to-ferrite transformation, additional systematic CCT tests were performed at a cooling rate of 1 °C/s using samples with a prior austenite grain size of 26 μm and different holding times at 900 °C. The measured kinetics of austenite decomposition, in terms of total fraction transformed versus temperature, is shown in Figure 7. It can be readily observed that the transformation shifts systematically to lower temperatures as the Nb content of austenite increases by decreasing the holding times at 900 °C from 20 to 6, 1 and 0 mins. Metallographic studies confirmed that polygonal ferrite constitutes more than 60% of the microstructure for all the examined cases.

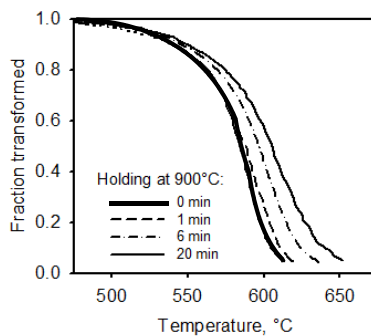


Figure 7. Effect of Nb in solution on the austenite decomposition kinetics in the X80 steel with a prior austenite grain size of 26 μm cooled at 1 °C/s.

Discussion

Transformation Start Model

The variation of Nb content in austenite due to Nb(CN) precipitation at 900 °C is too small to explain the observed effect on austenite decomposition in terms of the underlying thermodynamics, i.e. the driving pressure for transformation. Thus, Nb in solution is expected to affect kinetic factors, in particular the apparent mobility of the austenite-ferrite interface. For the delay in transformation-start also the effect of Nb on nucleation may be important, but a measurable transformation-start involves the early growth of ferrite grains. A ferrite-start model previously proposed for plain low carbon steels is being adopted here to analyze the role of Nb in the initial transformation stages [19]. The model considers early carbon diffusion controlled growth of ferrite grains nucleated at austenite grain corners at a temperature, T_N . The original model has been extended to include solute drag of Nb that slows down the growth rate of ferrite. The modified growth rate equation can be formulated as [20]:

$$\frac{dR_f}{dt} = D_C \frac{C^\gamma - C_o}{C^\gamma - C^\alpha} \frac{1}{R_f} \left(1 + \frac{D_C \alpha C_{Nb}}{R_f} \right)^{-1} \quad (1)$$

where R_f is the radius of the growing ferrite grain, D_C is the carbon diffusivity in austenite [21], C_o is the average carbon concentration, C^α and C^γ are the carbon equilibrium concentrations in ferrite and austenite, respectively, C_{Nb} denotes the concentration of Nb in solution and α is a constant related to the intensity of the solute-interface interaction. The carbon equilibrium concentrations are calculated with Thermo-Calc using the Fe2000 database and assuming ortho-equilibrium (i.e. full equilibrium for all alloying elements). Measurable transformation-start (i.e. 5% transformed) is assumed to be associated with nucleation site saturation at prior austenite grain boundary sites. Ferrite nucleation is presumed to cease once the carbon enrichment of the entire grain boundary area attains a critical level, C^* , i.e.:

$$R_f > \frac{1}{\sqrt{2}} \frac{C^* - C_o}{C^\gamma - C_o} d_\gamma \quad (2)$$

is the condition to calculate the transformation-start temperature, T_S . The three adjustable parameters, i.e. T_N , C^* and α , have been determined from the experimental ferrite transformation start temperatures as summarized in Table II. In this analysis, the parameter α that describes the role of Nb is similar in both steels that have comparable Nb levels. Also, the values for C^*/C_o fall in the same range for both steels but the apparent undercooling ($Ae3 - T_N$) for nucleation is much larger in the X80 steel, i.e. 123 °C vs 59 °C in the X65 steel. A possible reason for this difference may be that in the X65 steel Nb is the only microalloying element whereas the X80 steel also contains Mo and Ti. In particular, Mo delays the onset of ferrite transformation significantly.

Table II. Ferrite Transformation-start Parameters

Steel	T_N (°C)	C^*/C_o	α (s/μm)/(at.ppm)
X65	780	2.43	0.013
X80	700	$1.74 + 6.8\mu\text{m}/d_\gamma$	0.043

Apparent Austenite-Ferrite Interface Mobility

The overall kinetics of the formation of ferrite can be more rigorously analyzed to quantify the effect of Nb on the apparent austenite-ferrite interface mobility, M , for the investigated transformation scenarios. For this analysis, the formation of polygonal ferrite is considered. To this end, two main tasks have to be dealt with. Firstly, a suitable assumption for the growth geometry has to be established such that the interface velocity can be extracted from the measured transformation kinetics. Secondly, an appropriate kinetic model has to be adopted to interpret the interface velocity in terms of the interface mobility. As clearly seen in the micrograph shown in Figure 4(b), ferrite forms essentially as films along prior austenite grain boundaries and grows inwards to consume the austenite grain. A suitable geometry to describe this situation is a spherical austenite grain with an outer ferrite shell growing towards the grain interior [22]. This is relevant for cooling scenarios where nucleation site saturation occurs at

austenite grain boundaries and the overall kinetics is mainly controlled by subsequent thickening of the ferrite shell. The growth rate of ferrite in low carbon steels can be explained by a mixed-mode approach [22], in which the interface velocity, v_α , is related to the mobility term and the chemical driving pressure acting on the ferrite-austenite interface, $\Delta G_{\text{int}}^{\gamma \rightarrow \alpha}$, i.e.

$$v_\alpha = M \Delta G_{\text{int}}^{\gamma \rightarrow \alpha} \quad (3)$$

The driving pressure can be quantified based on the difference between the interfacial carbon concentration, C_{int}^γ , and the equilibrium carbon content of austenite, C_{eq}^γ , with respect to para-equilibrium. The assumed geometry and the carbon concentration profile during the transformation are illustrated schematically in Figure 8. The interfacial carbon concentration at the austenite side is *a priori* unknown in the mixed-mode growth scenario. It evolves with time and has to be determined by solving carbon flux equations across the interface and within the austenite. Numerical procedures have been proposed to self-consistently extract M and C_{int}^γ from this analysis [23,24].

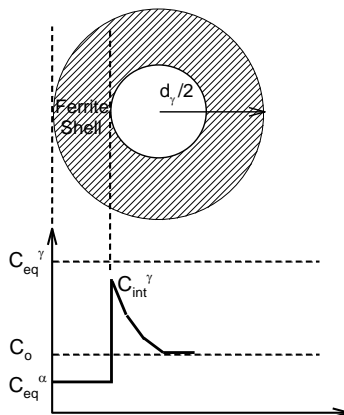


Figure 8. Schematic illustration of carbon profile within the domain consisting of a spherical austenite grain with an outer ferrite shell.

Figure 9 shows the apparent mobility in the X65 steel as a function of temperature for the ferrite portion of the CCT data shown in Figure 3. For a given temperature the apparent mobility decreases with increasing amount of Nb in solution. Interestingly, however, the apparent mobility decreases with increasing temperature. In the case with very little Nb remaining in solution it appears that a maximum of the apparent mobility is obtained at approximately 650 °C. The effect of cooling rate on apparent mobility is shown in Figure 10 for the situation that all Nb is in solution. Here, the occurrence of a maximum in the apparent mobility at an intermediate transformation temperature is clearly observed for lower cooling rates. Another striking feature of Figure 10 is that the apparent mobility is not only a function of temperature but also depends

on cooling rate. The observations for the apparent mobility are similar in the X80 steel, as illustrated in Figure 11. Clearly, the apparent mobility decreases with increasing Nb content in solution as well as with increasing temperature.

One may rationalize these findings considering a solute drag effect of Nb on the migrating austenite-ferrite interface. Classical solute drag models [25] predict that the solute drag effect increases with solute concentration. This is consistent with the observation that the apparent mobility decreases with increasing solute Nb content. Further, the solute drag pressure depends on the interface velocity and shows a maximum at intermediate velocity values. This may explain the surprising temperature trend and the effect of cooling rate on the apparent interface mobility. It will be important to conduct a rigorous solute drag analysis on the extracted mobility data following approaches previously applied to other low carbon steels (without Nb microalloying) and Fe-Mn alloys [26,27]. This will permit evaluation of whether or not classical solute drag theories lead to a consistent description of the effect of Nb in solution on the austenite-to-ferrite transformation. For the X80 steel, it will also be important to analyze more rigorously the synergistic role of Nb and Mo.

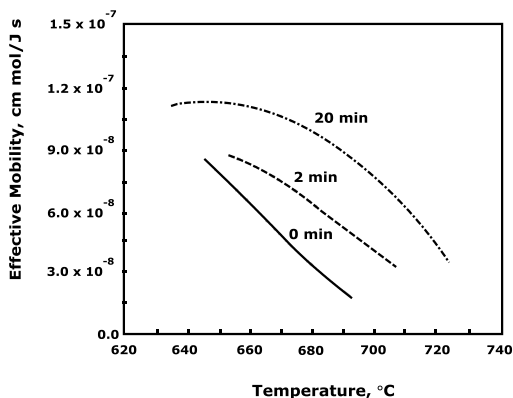


Figure 9. Effect of Nb in solution on effective mobility of austenite-ferrite interface in X65 steel cooled at 5 °C/s.

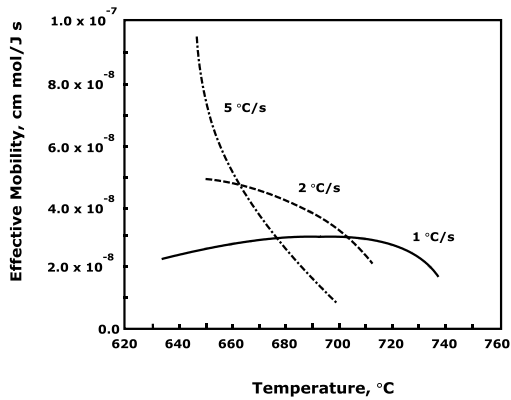


Figure 10. Effect of cooling rate on effective mobility of austenite-ferrite interface in X65 steel with all Nb in solution.

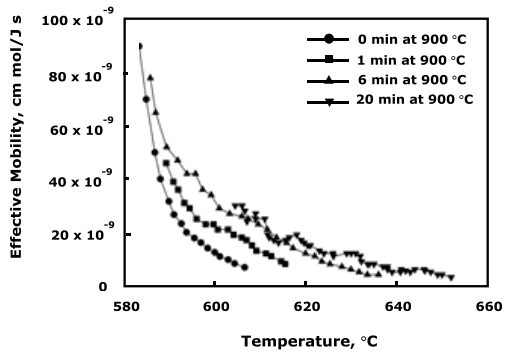


Figure 11. Effect of Nb in solution on effective mobility of austenite-ferrite interface in X80 steel with an austenite grain size of 26 μm cooled at 1 $^{\circ}\text{C/s}$.

Conclusions

This paper provides a renewed in-depth investigation of the solute drag effect of Nb and Mo on the austenite decomposition in linepipe steels. A particularly significant role of Nb is confirmed that is of paramount importance when thermo-mechanically processing or welding these steels as the amount of Nb in solution may vary as a function of the employed process path or welding conditions. Further, the synergistic effects of Nb with Mo require further detailed studies. It is proposed to employ a rigorous solute drag analysis to quantify the effects of Nb and/or Mo on the austenite-to-ferrite transformation. This analysis will have to be extended to the bainite transformation. Bainitic transformation products are increasingly sought in higher strength linepipe steels and other state-of-the-art high-strength steels. Preliminary studies for the X80 steel indicate that bringing Nb into solution has also a marked effect on the bainite transformation [28].

Acknowledgements

We acknowledge the financial support received from the Natural Sciences and Engineering Research Council of Canada, Evraz Inc. NA and TransCanada Pipelines Ltd. with gratitude. Further, we would like to thank Sepehr Gerami, Thomas Garcin and Jennifer Reichert for their assistance in experimental and analyzing work.

References

1. W.B. Morrison, "Microalloy Steels – The Beginning," *Materials Science and Technology*, 25 (9) (2009), 1066-1073.
2. A.J. DeArdo et al., "On Strength of Microalloyed Steels: An Interpretive Review," *Materials Science and Technology*, 25 (9) (2009), 1074-1082.
3. Y. Terada et al., "Development of API X100 UOE Line Pipe," *Nippon Steel Technical Report (Japan)*, 72 (1997), 47-52.
4. J.D. Jones and A.B. Rothwell, "Controlled Rolling of Low-carbon Niobium-treated Mild Steels," *Special Report*, 108, ISI, London (1968), 78.
5. I. Weiss and J.J. Jonas, "Interaction Between Recrystallization and Precipitation During the High Temperature Deformation of HSLA Steels," *Metallurgical Transactions A*, 10 (7) (1979), 831-840.
6. A. Yoshie et al., "Modelling of Microstructural Evolution and Mechanical Properties of Steel Plates Produced by Thermo-mechanical Control Process," *Iron and Steel Institute of Japan International*, 32 (1992), 395-404.
7. W.B. Morrison, "The Influence of Small Niobium Additions on the Properties of Carbon-manganese Steels," *Journal of the Iron and Steel Institute*, 201 (4) (1963), 317-325.

8. S. Okaguchi, T. Hashimoto, and H. Ohtani, "Effect of Niobium, Vanadium and Titanium on Transformation Behavior of HSLA Steel in Accelerated Cooling" (Paper presented at the International Conference on Physical Metallurgy of Thermomechanical Processing of Steels and Other Metals, THERMEC-88, Keidanren Kaikan, Tokyo 6-10 June 1988), (1) 330-336.
9. Y.J.M. Brechet et al., "Effect of Nb on Ferrite Recrystallization and Austenite Decomposition in Microalloyed Steels," *Steel Research International*, 78 (3) (2007), 210-215.
10. C. Fossaert et al., "The Effect of Niobium on the Hardenability of Microalloyed Austenite," *Metallurgical and Materials Transactions A*, 26 (1) (1995), 21-30.
11. Y. Takahama and J. Sietsma, "Mobility Analysis of the Austenite to Ferrite Transformation in Nb Microalloyed Steel by Phase Field Modelling," *Iron and Steel Institute of Japan International*, 48 (4) (2008), 512-517.
12. W.T. Reynolds Jr. et al., "The Incomplete Transformation Phenomenon in Fe-C-Mo Alloys," *Metallurgical Transactions A*, 21 (6) (1990), 1433-1463.
13. H.I. Aaronson, W.T. Reynolds Jr., and G.R. Purdy, "The Incomplete Transformation Phenomenon in Steel," *Metallurgical and Materials Transactions A*, 37 (6) (2006), 1731-1745.
14. H. Mohrbacher, "Mo and Nb Alloying in Plate Steels for High-performance Applications" (Paper presented at the The International Symposium on the Recent Developments in Plate Steels, AIST, Warrendale, PA, 19-22 June, 2011), 169-179.
15. P.A. Manohar et al., "Grain Growth Predictions in Microalloyed Steels," *Iron and Steel Institute of Japan International*, 36 (2) (1996), 194-200.
16. N. Isasti et al., "Effect of Composition and Deformation on Coarse-grained Austenite Transformation in Nb-Mo Microalloyed Steels," *Metallurgical and Materials Transactions A*, 42 (12) (2011), 3729-3742.
17. J.S. Park et al., "Dissolution and Precipitation Kinetics of Nb (C,N) in Austenite of a Low Carbon Nb-Microalloyed Steel," *Metallurgical and Materials Transactions A*, 40 (3), 2009, 560-568.
18. J.M. Gray, "Evolution of Microalloyed Linepipe Steels with Particular Emphasis on the 'Near Stoichiometry' Low Carbon, 0.10 Percent Niobium 'HTP' Concept," *Journal of Iron and Steel Research International*, 18 (1-2) (2011), 652-657.
19. M. Militzer, R. Pandi, and E.B. Hawbolt, "Ferrite Nucleation and Growth During Continuous Cooling," *Metallurgical and Materials Transactions A*, 27 (6) (1996), 1547-1556.
20. M. Militzer, F. Fazeli, and H. Azizi-Alizamini, "Modelling of Microstructure Evolution in Advanced High Strength Steels," *La Metallurgica Italiana*, (4) (2011), 35-41.

21. J. Ågren, "A Revised Expression for the Diffusivity of Carbon in Binary Fe C Austenite," *Scripta Metallurgica*, 20 (11) (1986), 1507-1510.
22. R.G. Kamat et al., "The Principle of Additivity and the Proeutectoid Ferrite Transformation," *Metallurgical Transactions A*, 23 (9) (1992), 2469-2480.
23. J. Sietsma and S. van der Zwaag, "A Concise Model for Mixed-mode Phase Transformations in the Solid State," *Acta Materialia*, 52 (14) (2004), 4143-4152.
24. F. Fazeli, "Modelling the Austenite Decomposition into Ferrite and Bainite" (Ph.D. thesis, The University of British Columbia, Vancouver, 2005).
25. J.W. Cahn, "The Impurity-drag Effect in Grain Boundary Motion," *Acta Metallurgica*, 10 (9) (1962), 789-798.
26. F. Fazeli and M. Militzer, "Application of Solute Drag Theory to Model Ferrite Formation in Multiphase Steels," *Metallurgical and Materials Transactions A*, 36 (6) (2005), 1395-1405.
27. T. Jia and M. Militzer, "Modelling Phase Transformation Kinetics in Fe-Mn Alloys," *Iron and Steel Institute of Japan International*, 52 (4) (2012), 644-649.
28. F. Fazeli et al., "Modelling the Effect of Nb on Austenite Decomposition in Advanced Steels" (Paper presented at The International Symposium on the Recent Developments in Plate Steels, AIST, Warrendale, PA, 19-22 June 2011), 343-350.